Aus dem Zentrum für Augenheilkunde der Universität zu Köln

Klinik und Poliklinik für Allgemeine Augenheilkunde

Direktor: Universitätsprofessor Dr. med. C. Cursiefen

A VISUAL OBSERVATION OF THE AGE DEPENDENCY IN THE UBM PARAMETERS WITHIN THE LOWER EYELID AND PERIOCULAR STRUCTURES

Inaugural-Dissertation zur Erlangung der Doktorwürde
der Medizinischen Fakultät
der Universität zu Köln

vorgelegt von
Xiaojun Ju
aus Chongqing, China

promoviert am 19.Mai 2025

Gedruckt mit Genehmigung der Medizinischen Fakultät der Universität zu Köln
2025

Dekan: Universitätsprofessor Dr. med. G. R. Fink

1. Gutachter: Universitätsprofessor Dr. med. Dr. phil. L. M. Heindl
2. Gutachterin: Privatdozentin Dr. med. T. Schick

Erklärung

Ich erkläre hiermit, dass ich die vorliegende Dissertationsschrift ohne unzulässige Hilfe Dritter und ohne Benutzung anderer als der angegebenen Hilfsmittel angefertigt habe; die aus fremden Quellen direkt oder indirekt übernommenen Gedanken sind als solche kenntlich gemacht.

Bei der Auswahl und Auswertung des Materials sowie bei der Herstellung des Manuskriptes habe ich Unterstützung von folgender Person erhalten:

Herr D. H. Kowanz

Weitere Personen waren an der Erstellung der vorliegenden Arbeit nicht beteiligt. Insbesondere habe ich nicht die Hilfe einer Promotionsberaterin/eines Promotionsberaters in Anspruch genommen. Dritte haben von mir weder unmittelbar noch mittelbar geldwerte Leistungen für Arbeiten erhalten, die im Zusammenhang mit dem Inhalt der vorgelegten Dissertationsschrift stehen.

Die Dissertationsschrift wurde von mir bisher weder im Inland noch im Ausland in gleicher oder ähnlicher Form einer anderen Prüfungsbehörde vorgelegt.

Die Einholung des Ethikvotums wurde von Herrn D. H. Kowanz übernommen. Die Erstellung des Studienprotokolls sowie die Rekrutierung der Probanden erfolgten gemeinsam durch Herrn D. H. Kowanz und mich. Die in dieser Arbeit beschriebenen Untersuchungen wurden nach der initialen Einführung eigenständig von mir durchgeführt und betreut. Zur Bestimmung der Interrater-Reliabilität wurden Wiederholungsmessungen jeweils von beiden durchgeführt. Die statistische Auswertung der Daten sowie die Erstellung der wissenschaftlichen Publikation erfolgten anschließend durch mich.

Erklärung zur guten wissenschaftlichen Praxis:

Ich erkläre hiermit, dass ich die Ordnung zur Sicherung guter wissenschaftlicher Praxis und zum Umgang mit wissenschaftlichem Fehlverhalten (Amtliche Mitteilung der Universität zu Köln AM 132/2020) der Universität zu Köln gelesen habe und verpflichte mich hiermit, die dort genannten Vorgaben bei allen wissenschaftlichen Tätigkeiten zu beachten und umzusetzen.

Köln, 03.07.2024

Unterschrift:

ACKNOWLEDGEMENTS

I sincerely thank all those who contributed to the completion of this doctoral thesis. First of all, I would like to express my deepest gratitude to my supervisor, Ludwig M. Heindl, for his valuable guidance, unwavering support and academic guidance throughout my three years of study. His expertise, encouragement, and constructive feedback were instrumental in shaping this research and my academic growth.

I would like to express my sincere gratitude to Alexander C. Rokohl, my other mentor during my doctoral study, for his insightful advice, critical evaluation, and dedication to excellence, which enabled the successful completion of my project.

I am sincerely grateful to my colleagues, friends and family for their unwavering encouragement, understanding and support throughout this challenging but rewarding journey. Their belief in me has always been a source of motivation and inspiration.

Finally, I would also like to thank myself for my persistence for making my research possible.

I dedicate this paper to all those who have contributed, however small, to my academic and personal growth. Your contributions will always be cherished and remembered.

Widmung

Für meine Eltern – ohne ihre Liebe und Unterstützung wäre dies nicht möglich gewesen.

TABLE OF CONTENTS

LIST OF ABBREVIATIONS

UBM: Ultrasound biomicroscopy

CT: Computed tomography

MRI: Magnetic resonance imaging

PTO: The pre-tarsal orbicularis

PSO: The pre-septal orbicularis

CPF: The capsulopalpebral fascia

DOL: The depressor orbicularis lateralis

BMI: Body mass index

ZUSAMMENFASSUNG

Die Ultraschall-Biomikroskopie (UBM) ist ein etabliertes Verfahren in der ophthalmologischen Diagnostik, wird jedoch vergleichsweise selten zur Untersuchung der Augenlider oder periokularen Strukturen eingesetzt. In dieser Studie wurden 42 gesunde Probanden (20 Männer, 22 Frauen; Alter 40,3 ± 19,9 Jahre) mit hochauflösender UBM (ABSOLU; Quantel Medical, Frankreich, 50 MHz) untersucht.

Untersucht wurden die wichtigsten anatomischen Strukturen des unteren Augenlids, darunter die Kapsulopalpebralfaszie (CPF), der prätarsale Orbicularis (PTO), die Tarsalplatte, der präseptale Orbicularis (PSO), der Bindehautkomplex sowie der Musculus depressor orbicularis lateralis (DOL). Während der Untersuchung wurden standardisierte Ultraschallbilder aufgenommen, und die Dicke der genannten Strukturen in Primärblick- sowie Aufblickposition mit dem ABSOLU-System analysiert und vermessen. Die Ergebnisse wurden statistisch ausgewertet.

Dabei wurde festgestellt, dass sich einige Strukturen des unteren Augenlids während dynamischer Augenbewegungen verändern, wobei sich die Dicke derselben Struktur an verschiedenen Messpunkten unterscheiden kann. Insbesondere zeigte der PSO im Aufblick eine signifikante Reduktion der Dicke. Darüber hinaus ließ sich ein Zusammenhang zwischen bestimmten Strukturen und dem Alter der Probanden beobachten: Einige Strukturen zeigten eine altersabhängige Zunahme der Dicke. Zudem waren einzelne Strukturen bei männlichen Teilnehmern dicker als bei weiblichen.

Aus dieser Untersuchung lässt sich schließen, dass die UBM eine sichere, nicht-invasive und effektive Methode zur Darstellung der Anatomie und altersbedingten Veränderung des unteren Augenlids darstellt. Diese Technologie ermöglicht neue Einblicke in die periorbitale Physiologie und Dynamik bei gesunden Personen und könnte darüber hinaus zur Beurteilung von Erkrankungen oder zur Evaluierung kosmetischer sowie chirurgischer Maßnahmen eingesetzt werden.

SUMMARY

Ultrasound biomicroscopy is a standard machine used for ophthalmic examinations, but its use on the eyelids or periocular area is less common. Our study examined 42 healthy volunteers using High-resolution ultrasound biomicroscopy (ABSOLU; Quantel Medical, France, 50MHz). We used ultrasound technology to explore the main structures of the lower eyelid, which include the capsulopalpebral fascia (CPF), the pre-tarsal orbicularis (PTO), the tarsal plate, pre-septal orbicularis (PSO), the conjunctiva complex, and the depressor orbicularis lateralis (DOL). During the examination, corresponding ultrasound images were captured, and the thickness of the layers of the lower eyelid at the primary gaze position and the up-gaze position were analyzed and measured using the ABSOLU system. The results were then statistically analyzed. At the same time, the images and data collected during the study were used to analyze the dynamic changes of the lower eyelid structure further when the gaze direction changes and its age-related variation. We collected and analyzed images of 42 volunteers taken by Ultrasound Biomicroscopy, including 20 men and 22 women (age 40.3±19.9 years old). Our study recorded different structure thicknesses of the lower eyelid in an eyeball movement in a healthy population, including the primary and up-gaze positions. We found that some structures of the lower eyelid change during dynamic eyeball movements, and the thickness of the same structure at various measurement points on the lower eyelid also varies. In terms of gender and age differences, some of the lower eyelid structures thicken with aging. Meanwhile, some parts of the lower eyelid structures in men are thicker than the corresponding structures in women.

From this study, we have drawn the preliminary conclusion that using ultrasonic biomicroscopy to safely and non-invasively examine the changes and morphology of the lower eyelid is an effective way to gain insight into the eyelid and its aging process. This technology is being used widely, enabling us to study periocular physiology and the dynamics of patients with certain diseases. In addition, it can be used to evaluate the effects of cosmetic and periocular surgery.

1. INTRODUCTION

Our research focuses on UBM observation and measurement of the lower eyelid and the analysis of its dynamic changes and age-related variations on the basis of ultrasound images. Therefore, we need to first gain an in-depth understanding of the anatomy of the lower eyelid, and propose new research directions for analysis based on previous clinical images of non-invasive examination of eyelid structure and previous research conclusions on eyelid aging.

1.1. Lower Eyelid Structure

The eyelid is a membrane skin fold located in front of the eyeball and divided into upper and lower parts, whose primary function is to cover and protect the eyeball. The structure of the lower eyelid, from the inner layer to the outer layer, consists mainly of the innermost layer of orbital adipose tissue, subcutaneous fascia, the orbicularis oculi muscle, subcutaneous fat, and skin. In terms of specific structures, the eyelid is divided into three layers: posterior, middle, and anterior.[1] The posterior layer includes the tarsal plate, orbicularis oculi muscle, and conjunctiva. The middle layer refers to the combination of the orbital septum, orbital fat, and infraorbital fibrous adipose tissue. The anterior layer includes the orbicularis oculi muscle and skin.[2] **Figure 1** shows the structure of each layer of the lower eyelid. Furthermore, the

corresponding structures of the eyelid, particularly the lower eyelid, are described in detail below.

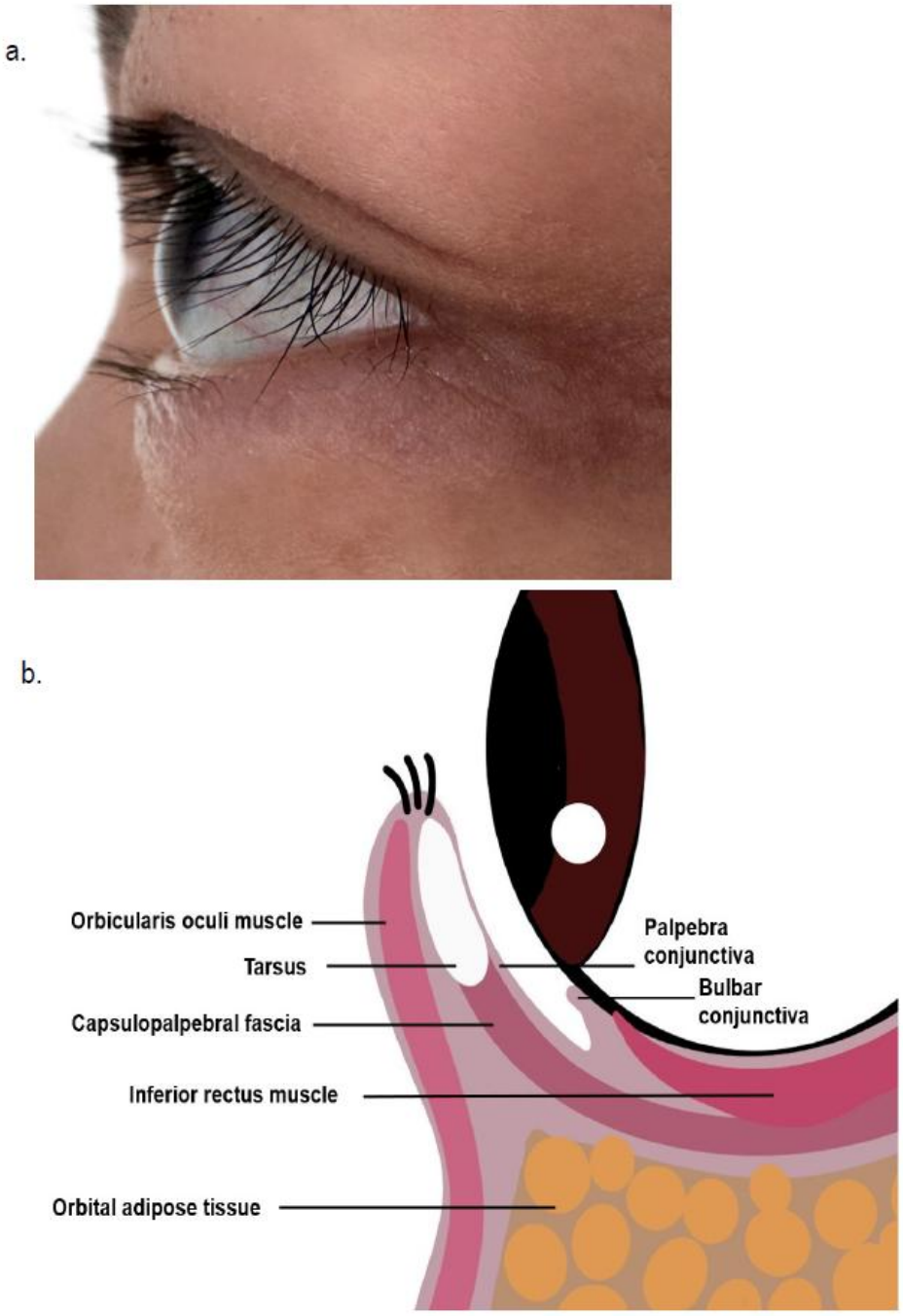

(**Figure 1.** a. Lower eyelid appearance. b. Lower eyelid layers.)

1.1.1. Skin/Subcutaneous Tissue

The eyelid skin is the outermost structure of the lower eyelid, and the structure is visible in the appearance. The skin of the lower eyelid has a unique anatomical feature that distinguishes it from other structures. This is because it does not have subcutaneous fat, which makes it one of the thinnest skin layers in the body. With an average thickness of about 0.6 millimeters, eyelid skin is particularly prone to wrinkle formation, reflecting its delicate nature.[3] The subcutaneous tissues are composed of fatty cells and loose connective tissue. This combination provides a degree of flexibility and mobility that is essential for the complex movements of the eyelid. The margin of the eyelids is the boundary between the outer layer of the eye and the inner layer of the eye. Thus, this area, as a transition zone between the delicate structures in the eye and the external environment, serves as a boundary that helps maintain the function and structural integrity of the lower eyelid.[4] Overall, the eyelid skin serves as an essential protective shell for the eyeball, combining the triple functions of defense and motion as well as appearance, and is the basis for our observation and research of the aesthetics of the periocular area and related research.

1.1.2. Muscles

The lower eyelid performs a variety of eye movements and functions that are accomplished with the assistance of its major muscles. Among the more common and typical behaviors of the lower eyelid are blinking (autonomous, spontaneous, or reflexive), eye closing (voluntary or forced), partial drooping of the eyelid during squinting, normal contraction of the eyelid in response to emotional states such as surprise or fear (startle reflex), and coordinated vertical eye movements, which provide maximum protection for the eye.[5,6]

The lower eyelid is less mobile than that of the upper one. The dominant muscle for movement control in the lower and upper eyelids is called orbicularis. This muscle is situated beneath the skin's surface.[7] Anatomically, it is composed of three separate segments as the most functional eyelid muscle: the anterior segment of the septum, the anterior segment of the levator palpebralis, and the orbital segment. The various anatomical segments of the lower

eyelid are responsible for controlling the different functions and activities of the eye. The anterior septal segments and the anterior segment of the levator palpebralis are responsible for the involuntary blinking, and the orbital segment is responsible for the forced/voluntary eyelid closure.[8] The upper orbicularis oculi muscle and the lower orbicularis oculi muscle are responsible for covering the upper and lower lids' tarsal bones, respectively.[9] Further anatomical analysis revealed that the medial portion of the prestental orbicular oculi muscle can be divided into two head structures: the superficial head and the deep head. The superficial head of the muscle is attached to the anterior limb of the medial canthal ligament. In contrast, the deep head of the muscle is attached to the fascia surrounding the lacrimal sac and the posterior lacrimal ridge. The superficial and deep heads of the pretarsal orbicularis oculi muscle are similar to those found in the medial aspect of this muscle. The attachment to the posterior lacrimal crest and the medial canthal tendon is deep, while the attachment to the anterior lacrimal crest is superficial.[10] In addition, the deep head of the preticularis oculi muscle, which is also known as Horner's muscle, is located on the posterior part of the muscle.[11] The lateral canthal tendon is attached to the Horner muscle, which also serves as a component of the lacrimal apparatus. It allows the tissues to drain tears.[11]

The orbicularis muscles' junction of the upper and lower lids has a noteworthy feature that involves a portion of the muscle that moves vertically on the lateral aspect of the orbicularis oculi muscle.[9] This muscle, which is called the lateral descending muscle of the orbicularis oculi, has a prominent brow-lowering effect. Lemke et al.[12] identified this muscle when exploring the mechanism of brow ptosis. They found a vertical muscle fascicle prevalent adjacent to the lateral side of the orbicularis oculi muscle by dissecting human samples. In their study, they named it vertical lateral orbicularis fibers and proposed that this vertical structure may play an important role in forming brow ptosis and crow's feet. With the continuous clinical exploration and anatomical study of brow ptosis correction surgery, the muscle has been further defined in the literature. Tamatsu Y et al.[13] elucidated that this muscle fiber is comparatively separated from the lateral orbicularis oculi muscle, that it begins at the medial orbicularis ligament, moves in an arc around the lower lid margin, is almost perpendicular to

the medial and lateral canthus, and terminates in the subcutaneous tissue to the lateral orbicularis oculi ligament. Its width (4.90 ± 2.58) mm is a clear reflection of the aging of the tail of the eye and has a strong brow-lowering effect.

Moreover, there are some muscles in the lower eyelid that assist in the function of the lower eyelid. The bleb fascia resembles the membrane of the upper lid's levator tendon. Its fibers originate from the inferior rectus muscle, which can form the ligament of Lockwood.[14] In addition, the lower eyelid also has a levator muscle like the one found in the upper one, similar to the Müllerian muscle of the upper eyelid. It is underdeveloped and is located just posterior to the lower lid's capsular fascia.[10]

1.1.3. Tarsus

Tarsal plates are important components of the lower eyelids. Compared to the upper one, the size of the lower one's tarsal plate is smaller. The eyelash follicles and meibomian glands are included in the tarsal plate. It is composed of dense connective tissue.[15] Functionally, the meibomian glands it contains play a major role in secreting the oil layer, slowing down evaporation of the aqueous layer, and maintaining the surface tension of the tear film.[16] Meanwhile, the eyelash follicles provide “soil” for eyelash growth and play an essential role in protecting the ocular surface.[17] Anatomically, the horizontal length of the upper and lower tarsal plates is approximately 29 mm. Meanwhile, the length of the tarsal plate of the upper eyelid perpendicular to the center of the eyelid is 10 to 12 millimeters, whereas the length of the tarsal plate of the lower eyelid perpendicular to the center of the eyelid is at most 4 millimeters.[18] Regarding the tissue structure, according to literature records, there are about 30 meibomian glands on the upper eyelid and 100 eyelashes divided into 2 or 3 rows. There are about 20 meibomian glands and 50 eyelashes on the lower eyelid, most of which are arranged in a single row.[7,19] The rigid attachment of the two tarsals to the periosteum is maintained through the lateral and medial canthal tendons. Along with the meibomian glands, arranged parallel to and behind the eyelash line, the Zeis and Moll glands are associated with the eyelash follicles, secrete lipids and modify sweat, respectively.[20]

1.1.4. Conjunctiva

The innermost structure of the lower eyelid, known as the blepharon-conjunctiva, is an important part of the ocular anatomy and plays a key role in maintaining ocular health and function.[21] The lower eyelid blepharon-conjunctiva consists of a thin layer of mucous membrane that covers the inner surface of the lower eyelid, with the tarsal plates as the posterior boundary, extending forward to cover the front surface of the eyeball (also known as the bulbar-conjunctiva) until the edge of the cornea.[22] This transparent membrane consists mainly of stratified columnar epithelium interspersed with a small amount of connective tissue that gives the structure its elasticity and flexibility. The lining of the eyelid is characterized by a layer of nonkeratinized squamous epithelium that transitions seamlessly into the conjunctival epithelium that covers the ocular surface. Within the conjunctiva are accessory lacrimal glands and specialized mucus-secreting goblet cells, which play a vital role in maintaining the ocular tissues' delicate condition and preventing them from drying out.[23] This intricate network of structures emphasizes the important role of the lid conjunctiva in maintaining the integrity of the eye and facilitating the smooth functioning of the ocular surface.

1.2. Methods of Eyelid Thickness Measurement

The eyelid is only a tiny part of the human body, and its anatomy is even tinier. Understanding and mastering the anatomy of the eyelid is the basis for using non-invasive tools for observation and measurement. In previous clinical activities, we have also tried to use different measurement tools and observation equipment in the eyelid region.

Previous exploration and measurement of the morphology and thickness of various lower eyelid structures were mostly based on intuitive cadaver anatomy.[24,25] This method requires specimens of lower eyelid tissue to be dehydrated, embedded in paraffin, and cut into 7 μm-thick sagittal sections. After staining with Masson's trichrome, micrographs were taken using a digital camera system connected to the microscope.[26] Then measure through the post-production pictures. Direct anatomical observation is intuitive and precise, but cannot be quantified and extended to clinical routine and follow-up. In clinical practice, we mainly use

computed tomography (CT) and magnetic resonance imaging (MRI) to observe and measure the relevant structures internally in patients' eyelids.[27,28] However, this method is not convenient and expensive for local eyelid structures. At the same time, the structural changes of the eyelids under dynamic morphology cannot be observed.

1.3. Aging of the Lower Eyelid

As life expectancy increases globally, progressive and chronic eye diseases are becoming increasingly important in the ophthalmic disease spectrum.[29] Major eyelid pathology resulting from age-related degenerative changes include skin laxity, ectropion and entropion, and aponeurotic ptosis.[30] Further loss of laxity and tone is characteristic of aging of the eye accessory tissues, leading to eyelid ptosis.[31,32] Genetic causation is part of the intrinsic aging mechanism and cannot be changed by human behavior. However, outward aging can be the result of factors such as alcohol consumption, long-term exposure to the sun, smoking, and nutrition.[33,34]

The tissue structures of the lower eyelids change as people get older. This causes the overall appearance of their lower eyelids to become older.[35] Anterior displacement of orbital fat accompanied by relaxation of anchoring structures, such as aging of the orbicularis muscle and skin, are all associated with the overall aging process of the lower eyelid, and many of these factors often lead to serious periocular aging, in addition.[36] The various age-related changes that affect the lower eyelids' tissue structures can be seen in their individual characteristics. For instance, changes in the thickness and location of fat and muscle, especially the emergence of an orbital fat bulge and furthermore an alteration of its location.[37]

Aging around the lower eyelids causes many remarkable changes in appearance. The formation of the periorbital wrinkles or lateral canthal lines, which are also referred to as crow's feet, occurs at the upper and lower eyelids' junction. The formation of crow's feet mainly refers to the sagging of the lateral eyebrows and aging skin changes from a static aspect, while the dynamic expression of crow's feet is mainly due to the repeated contraction of the orbicularis

oculi muscle [38]. In addition, crow's feet are also caused by the combined effects of intrinsic aging (such as thinning of the eyelid skin and hypertrophy of the orbicularis oculi muscle) and extrinsic aging (such as repeated and significant facial expressions, especially eye expressions). [39] Pouches are facial phenomena of aging characterized by loose skin underneath the eyelids as well as fat swelling and hypertrophy of the lower orbicularis muscle.[40] And in particular this swelling of the lower eyelid or the appearance of "eye bags" due to aging is a major concern for patients seeking cosmetic evaluation and attention to facial rejuvenation.[41] A well-defined understanding of the various age-related changes affecting the lower eyelids can help enhance the results of lower orbital and cosmetic surgery.

In general, the morphological changes of the lower eyelids and even the periocular region caused by aging will not only cause physiological or pathological chronic eye diseases, but also cause a decrease in the aesthetic appearance. Therefore, both ophthalmologists, plastic surgeons, and the field of aesthetics need to monitor and evaluate the aging pattern around the eyes. In clinical applications, choosing appropriate tools and methods is also a current problem.

1.4. Ultrasound Biomicroscopy

Before introducing UBM in detail, **Figure 2** shows the complete UBM equipment currently in clinical use, which can provide an intuitive initial impression of the instrument. Overall, it consists of a host computer, a mechanical linear scanning probe, a display, a cart, a foot switch, an isolated power supply, and an external computer image processing software.

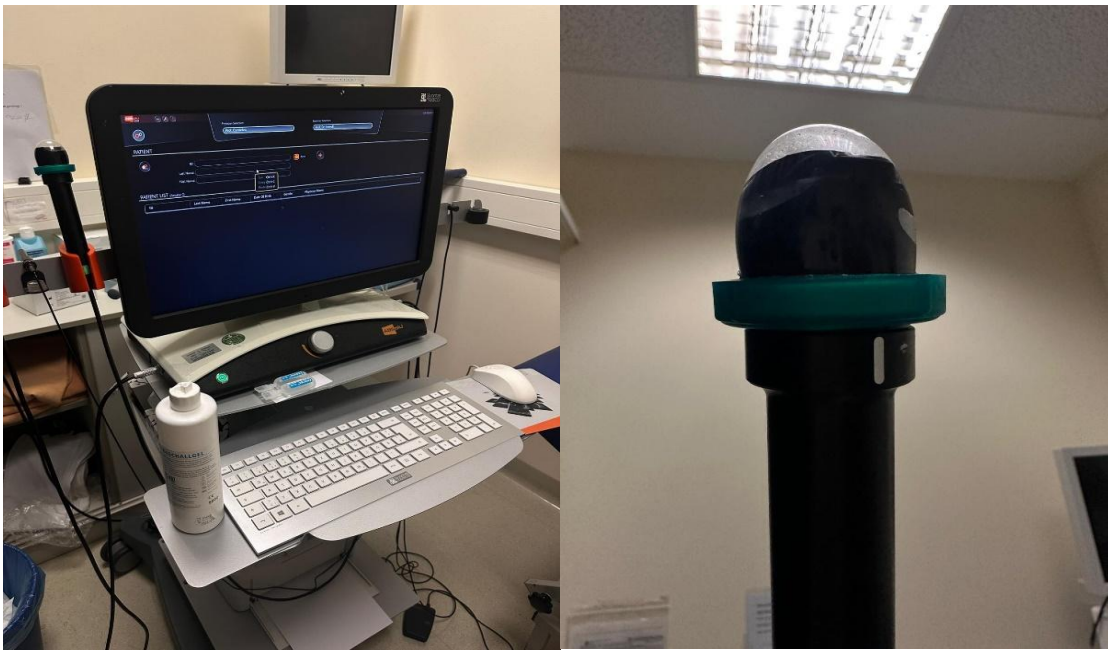

(**Figure 2.** Ultrasound biomicroscopy with 50 MHz probe) (ABSOLU; Quantel Medical, France)

1.4.1. Origins of ultrasound Biomicroscopy

Ultrasonic biomicroscopy (UBM) is a non-invasive imaging modality, which can visualize in-situ tissue sections with microscopic resolution. UBM uses high-frequency sound waves (35–100 MHz), and images with a depth of up to 4 mm and a resolution of 40–50 μm can be generated. High-frequency probes can provide a better and more accurate visualization of the subsurface structures and enable higher resolution even when there is pathological or anatomical occlusion.[42,43]

Under the principle of ultrasound physics, the quality of the image obtained by an ultrasound instrument on three aspects: the ultrasound frequency, the ratio of focal length to transducer diameter (focal length number), as well as the pulse length.[44] In general, the higher the frequency and the shorter the focal length, the higher the image resolution, but the poorer the penetration. For example, an ultrasound device with a short focal length (ca.1.2 mm) and a high frequency (80 MHz) can provide a very clear image, showing the epithelium with a resolution of 50 microns, but deeper structures may not be clearly displayed, and vice versa. A low-frequency (20 MHz) ultrasound image can penetrate deeper tissue and form an image,

but the image will be blurry. Then, the ultrasonic frequencies and focal lengths used at different measurement points or observation targets need to be constantly tried and explored. **Table 1** shows the differences and characteristics of different ultrasound frequencies in clinical use.

Table 1. Characteristics of Different Ultrasound Frequencies

Ultrasonic Frequency	Depth of Penetration	Imaging Structure
20MHz	10-15 mm	Dermis, Subcutaneous tissue
50MHz	4 mm	Dermis
80MHz	2 mm	Mucosal epithelium, Subepithelial elastic fibrous layer

1.4.2. Application of Ultrasound Biomicroscopy in Ophthalmology

The development of ultrasound for medical imaging of the ocular region can be traced back to the work of Mundt and Hughes [45] (A-scan), Greenwood and Mundt [46] (B-scan) in the 1950s. However, the center frequency of ophthalmic ultrasound equipment has almost always remained at or close to 10 MHz since the inception of the technology, resulting in unclear images due to low resolution. The frequency used by UBM (35-50 MHz) is significantly higher than that of traditional ophthalmic B-scanners. The resolution is improved to 40 mm or less, which brings the various ultrasound indicators of UBM closer to satisfying the standards of ideal imaging equipment.[47]

UBM offers two-dimensional images of the structures located in the anterior segment. This allows physicians to simultaneously view these anatomical features, which would be possible with a living eye. Live images are displayed on a video monitor and can be recorded for qualitative and quantitative analysis.[48] UBM was initially widely used in diagnosing and treating various types of glaucoma in the clinical field of ophthalmology because it has significant

advantages in observing front depth and angle conditions.[49,50] In addition, the clinicians and researchers were able to perform in-depth observations and examinations of the ciliary body and anterior chamber angle using UBM, which can be further utilized to record and evaluate the procedures related to anterior chamber tumor and lens surgery.[44]

Previous studies have attempted to use this tool to examine normal lower eyelid structures.[51,52] Similarly, our previous study also verified the reliability and accuracy of UBM in measurements of the upper eyelid structure.[53] In recent years, clinicians have gradually begun to use UBM to measure and record periorbital structures and eyelid tumors. Simultaneously, they have found that ultrasonic biomicroscopy can accurately measure the depth of eyelid lesions and obtain clear ultrasound images, which can be used as a basis for more accurate determination of tissue characteristics.[54]

1.5. Questions and aim of the work

Building upon the aforementioned context, it becomes imperative to delve into the crucial question of whether UBM holds the capacity to accurately measure and explore intricate periorbital structures. Additionally, it prompts an exploration into whether UBM can effectively capture age-related dynamic changes within the eyelid structure.

Given the intricate nature of periorbital anatomy, including delicate structures such as the tarsal plate, pre-tarsal orbicularis, and capsulopalpebral fascia, the accuracy and reliability of UBM measurements become paramount. By leveraging the high-resolution imaging capabilities of UBM, researchers can potentially attain unparalleled insights into the morphology and dynamics of these structures. This, in turn, can significantly augment our understanding of various ocular pathologies, as well as contribute to the refinement of surgical interventions targeting the periorbital region.

Moreover, UBM's ability to provide real-time imaging facilitates the observation of dynamic changes occurring within the eyelid structure over time. This opens up exciting avenues for investigating age-related alterations, such as changes in tissue elasticity, muscular integrity,

and overall structural integrity. By longitudinally tracking these dynamic changes across different age cohorts, researchers can gain valuable insights into the physiological aging process of the eyelids and its implications for ocular health.

The objective of this study is to provide an ultrasonographic analysis of the lower eyelids using UBM and also study the dynamics of these structures at different gaze positions. Specifically, we analyzed the pre-tarsal orbitalis (PTO), pre-septal orbitalis (PSO), the capsulopalpebral fascia (CPF), the tarsal plate, and the conjunctiva complex, as well as the depressor orbicularis lateralis (DOL) and their correlations in age-related changes. The ability to visualize the dynamic anatomy of the lower eyelid using ultrasound has helped improve our knowledge about the physiology of lower eyelid motility. This knowledge is fundamental to understanding the anatomical, structural, and functional changes in the eyelid aging process and lower lid-related diseases. It basically provides the data reference for the development of cosmetic periocular surgery, diagnosis of periocular deformities, and corrective eyelid surgery.

2. MATERIALS AND METHODS

2.1. Materials

2.1.1. Subjects

From June to December 2022, a comprehensive series of ultrasound biomicroscopy (UBM) examinations were conducted on the lower eyelids of 42 healthy individuals at the prestigious University Hospital of Cologne in Germany. This study was approved by the University of Cologne's Ethics Committee (approval number: 22-1202), and conducted under the highest ethical standards. It was also aligned with the principles of the Declaration of Helsinki. Prior to the commencement of any procedures, explicit consent was obtained from each participant, affirming their willingness for the publication of both their data and accompanying images. This unwavering commitment to ethical practice underscores the integrity and transparency of the study, ensuring the protection of participants' rights and privacy throughout the research process.

2.1.2. Inclusion Criteria

(a) All volunteers were between the ages of 18 and 87.

(b) All volunteers had intact eyelid structures in both eyes.

(c) All volunteers had normal eye movements in both eyes.

2.1.3. Exclusion Criteria

(a) Anyone with incomplete eyelid structure and a history of eyelid surgery.

(b) Those who are unable to gaze at one place normally.

(c) Those who cannot lie down.

(d) Those who are allergic to UBM probes.

(e) Unable to cooperate with inspectors.

2.2. Method

2.2.1. UBM Image Acquisition

For UBM image acquisition of the lower eyelid for volunteers, we refer to our previous successful experience with upper eyelid ultrasound image acquisition.[53] Participants were asked to provide their various characteristics, such as age, gender, past illnesses, and surgical history. One of the observers (Xiaojun, Ju. X.J.) then measured their height and weight using standardized protocols. BMI was then calculated based on the weight/height^2 (kg/m^2). The lower eyelids of volunteers were imaged using UBM (ABSOLU; Quantel Medical, France), equipped with a 50 -MHz contact linear probe (ABSOLU; Quantel Medical, France), and the ultrasound parameters were set (Gain: 105dB; Dyn: 50dB; TGC: 10dB). Each measurement point was measured twice for each volunteer (Donimik, Krowanz. D.K. twice). while ultrasound images of the lower eyelid were obtained and measured (Axial resolution: 35μm; Lateral resolution: 60μm). For the study, the volunteers were placed in a supine posture. They were shown two different gaze positions as we examined their lower eyelids. The first gaze position allowed them to look straight ahead, while the second gaze position allowed them to look upward. We then took images of the structures in the lower eyelid in their two gaze positions using standard and clear ultrasound images. **(Figure 3)**

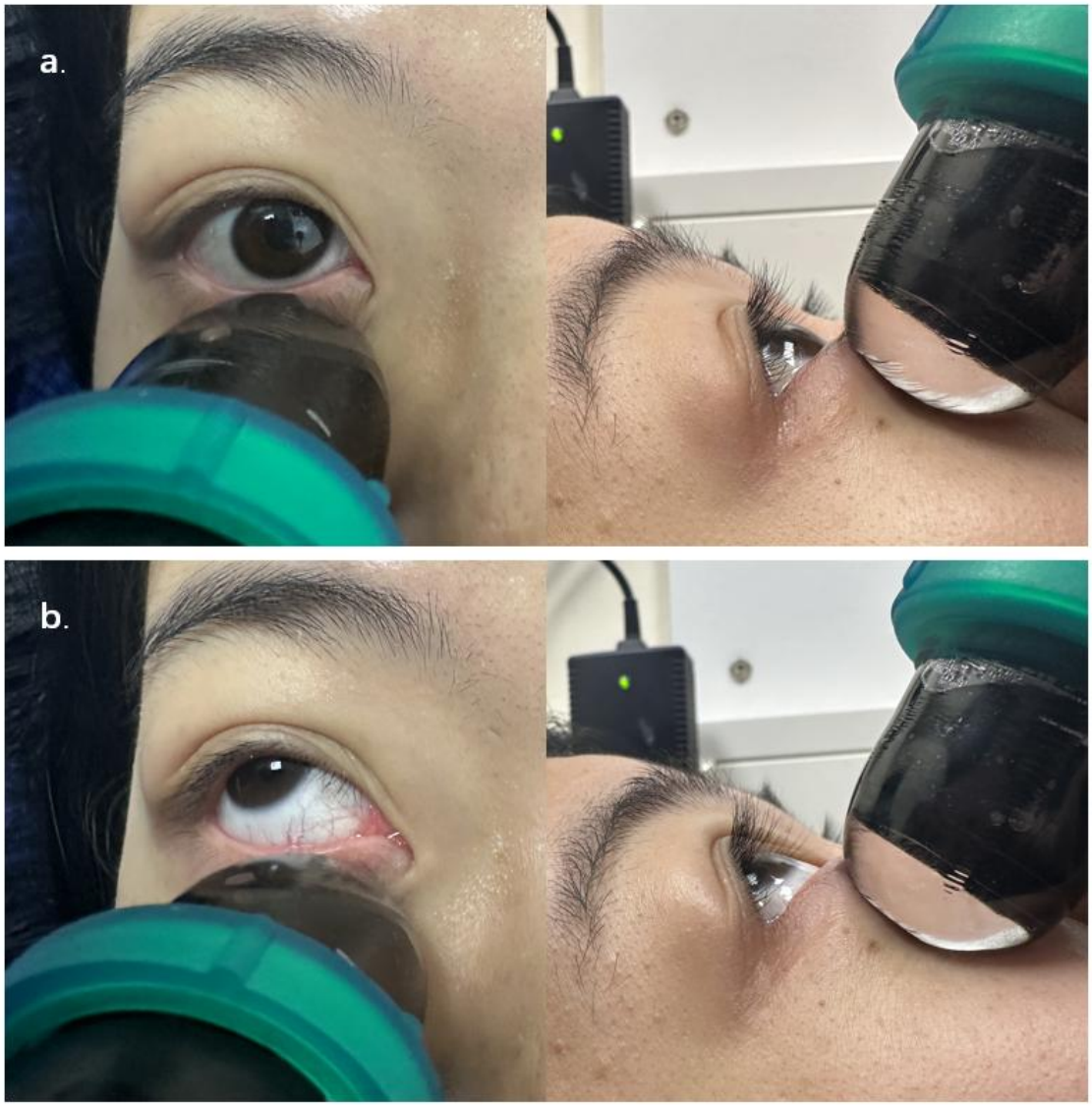

(**Figure 3. a.** Lower eyelid measurement at the primary gaze position using a 50 MHz UBM probe. **b.** Lower eyelid measurement at the up-gaze position using a 50 MHz UBM probe.)

The probe was then placed perpendicular to the lower eyelid margin. Scans were performed along the following 7 points: there are two measurement points at the primary gaze position, the pupil midline point and the eyebrow tail point at the primary gaze position, and for the up-gaze position, a total of five measurement points, the medial canthus point, the pupil midline point, the lateral canthus point, the medial pupil line point and the lateral pupil line point **(Figure 4)**. The detailed measurement points are shown in **Figure 4**. If there is a deviation

during the measurement, multiple measurements will be taken to correct it.

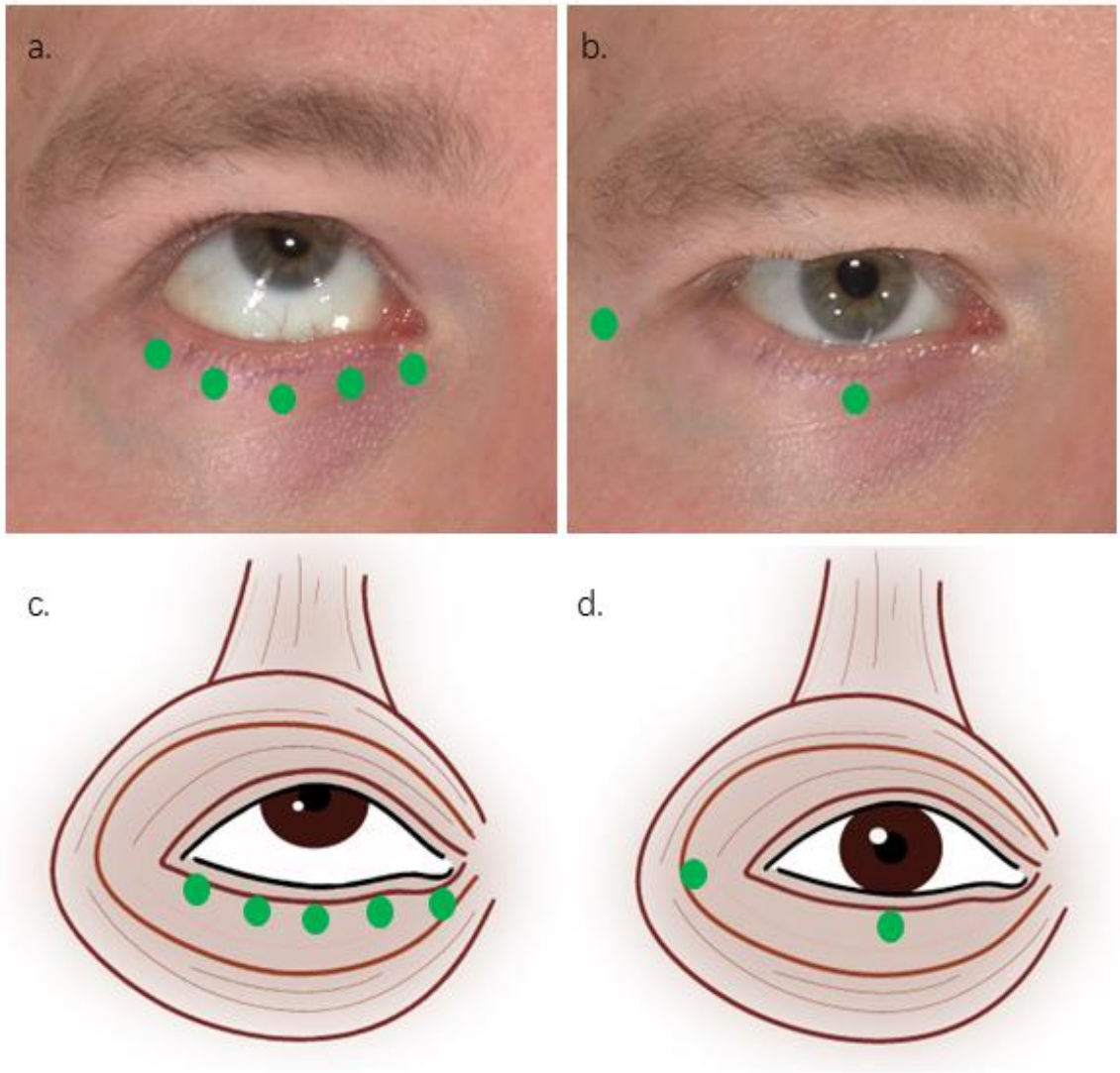

(**Figure 4.** The landmarks in the figure are from right to left: **a.** The medial canthus point, the medial pupillary line point, the pupillary midline point, the lateral pupillary line point, and the lateral canthus point at the up-gaze position. **b.** The pupillary midline point, the eyebrow tail point at the primary gaze position. **c.** The medial canthus point, the medial pupillary line point, the pupillary midline point, the lateral pupillary line point, and the lateral canthus point at the up-gaze position. **d.** The pupillary midline point, the eyebrow tail point at the primary gaze position.)

2.2.2. UBM Image Measurement

The measurement process of all ultrasound biomicroscopy (UBM) images was meticulously conducted using the ABSOLU image measurement system, a sophisticated tool equipped with linear measurement functionalities. This system enabled precise measurements directly on the ultrasound images, with linear measurement tools positioned perpendicular to each plane, facilitating accurate assessments in millimetres. Referring to the previous experience of UBM for the exploration of the lower eyelid structure, [52] two independent observers then distinguished and recorded (a) the type of echogenicity (hypoechoic or hyperechoic) of the different eyelid structures and (b) the thickness of the eyelid structures in millimeters, such as the pre-tarsal orbicularis (PTO), pre-septal orbicularis (PSO), the tarsal plate, the conjunctiva complex, the capsulopalpebral fascia (CPF) and the depressor orbicularis lateralis (DOL). Then, observers extracted static images of each measurement point and used ABSolu software to measure and describe the anatomical shape and character of the eyelid during different eyeball movement phases.

2.2.3. Reliability Analysis

To assess the reliability of the measurements, two independent raters, designated as rater 1 (Donimik, Krowanz. D.K.) and rater 2 (Xiaojun, Ju. X.J.), performed image measurements and analyses separately. Rater 2 (X.J.) conducted measurements and analyses on images captured on two occasions to evaluate intra-rater reliability. Meanwhile, the measurements obtained by the two raters were compared to evaluate inter-rater reliability. Intra-class correlation coefficients (ICC) were used to grade the reliability. If ICC<0.40, it is considered to be a poor agreement; if 0.40≤ICC<0.75, it is considered to be a satisfactory agreement; if 0.75≥ICC, it is considered to be an excellent agreement. Simultaneously, the measurement results were further analysed using paired t-test for reliability. The significance level of the data at *p-value* < 0.05 was regarded as statistically significant.

2.2.4. Statistical Methods

The data collected during the study were then analysed using the IBM SPSS Statistics 28 (Armonk, NY: IBM Corp.). All figures were produced using the GraphPad Prism 8.0.1 (GraphPad Software, San Diego, CA, USA), while the hand-drawn anatomical diagrams were created using Procreate Software. To verify normal distribution, the Kolmogorov–Smirnov test was used. The paired Wilcoxon test was also utilized to analyse the lower lid's thickness variation when the gaze position had changed. The study's results were analysed using the Friedman test to determine whether the tissue thickness at different measurement points was statistically different. Furthermore, we compare the variability between genders using the Mann-Whitney U test. The BMI and age correlation coefficient were also analysed using the Spearman correlation method.

The presented data collected during the study were analyzed using mean ± standard deviation (SD) to measure central tendency and variability. The significance level of the data at $p < 0.05$ was regarded as statistically significant, which indicated that the researchers had a low chance of getting the results through chance. This stringent criterion helped ensure the reliability and validity of the statistical findings in the study.

3. RESULTS

3.1. Reliability

According to our evaluation of ICC value, most of the inter- and intra-rater values were over 0.75, demonstrating excellent consistency. Only the measurements at capsulopalpebral and tarsus were between 0.40 and 0.75, and the inter-rater DOL measurement values reached satisfactory consistency (**Figure 5**).

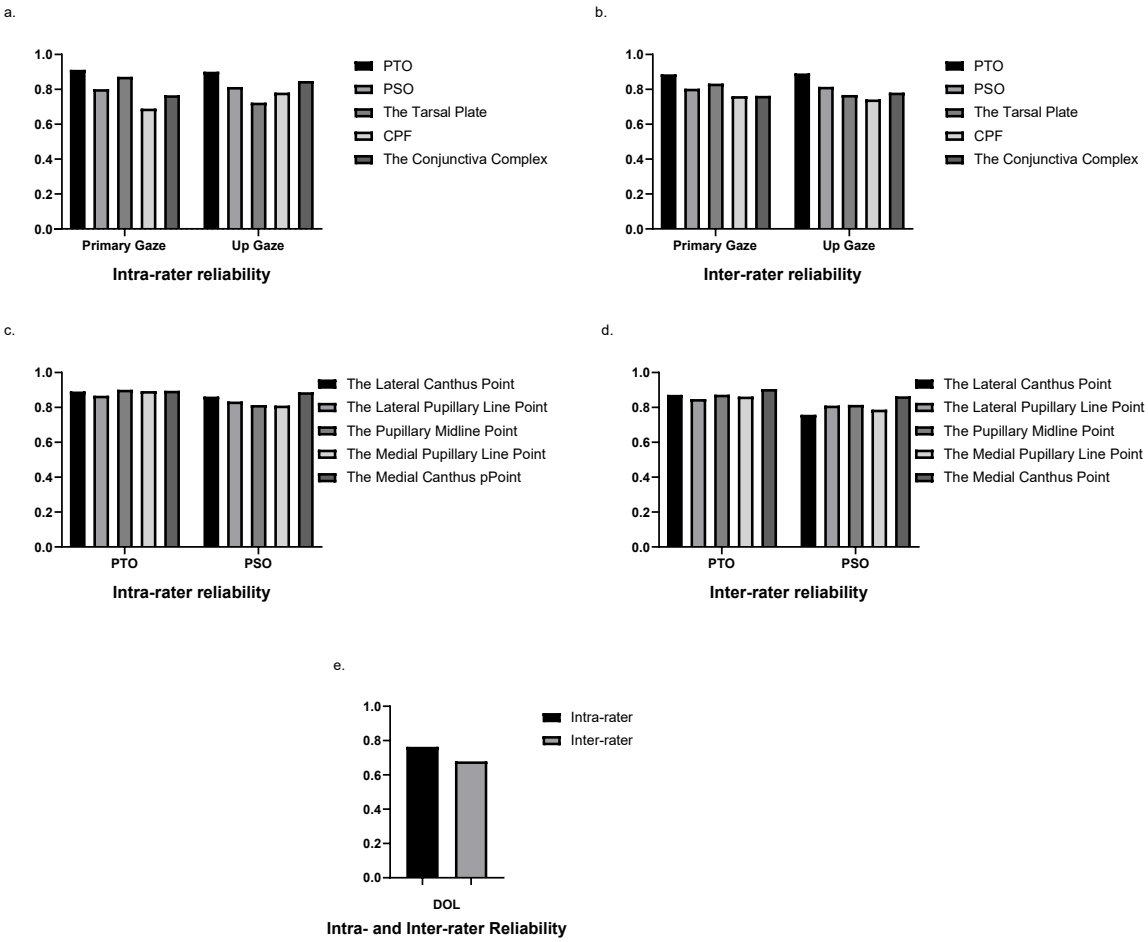

(**Figure 5 a.** The intraclass correlation coefficient for intra-rater at different gaze positions. **b.** The intraclass correlation coefficient for inter-rater at different gaze positions. **c.** The intraclass correlation coefficient for intra-rater at different measurement positions. **d.** The intraclass correlation coefficient for inter-rater at different measurement positions. **e.** The intraclass correlation coefficient for inter-and intra- rater for the thickness of the depressor orbicularis lateralis.)

Further, a paired t-test was performed on the intra- and inter-rater measurement values. At the up-gaze position, the intra-rater PTO measurement values were statistically different (p<0.05); Similarly, at the up-gaze position, the inter-rater PSO measurement values were statistically different (p<0.05). The remaining values were not statistically different (**Figure 6**).

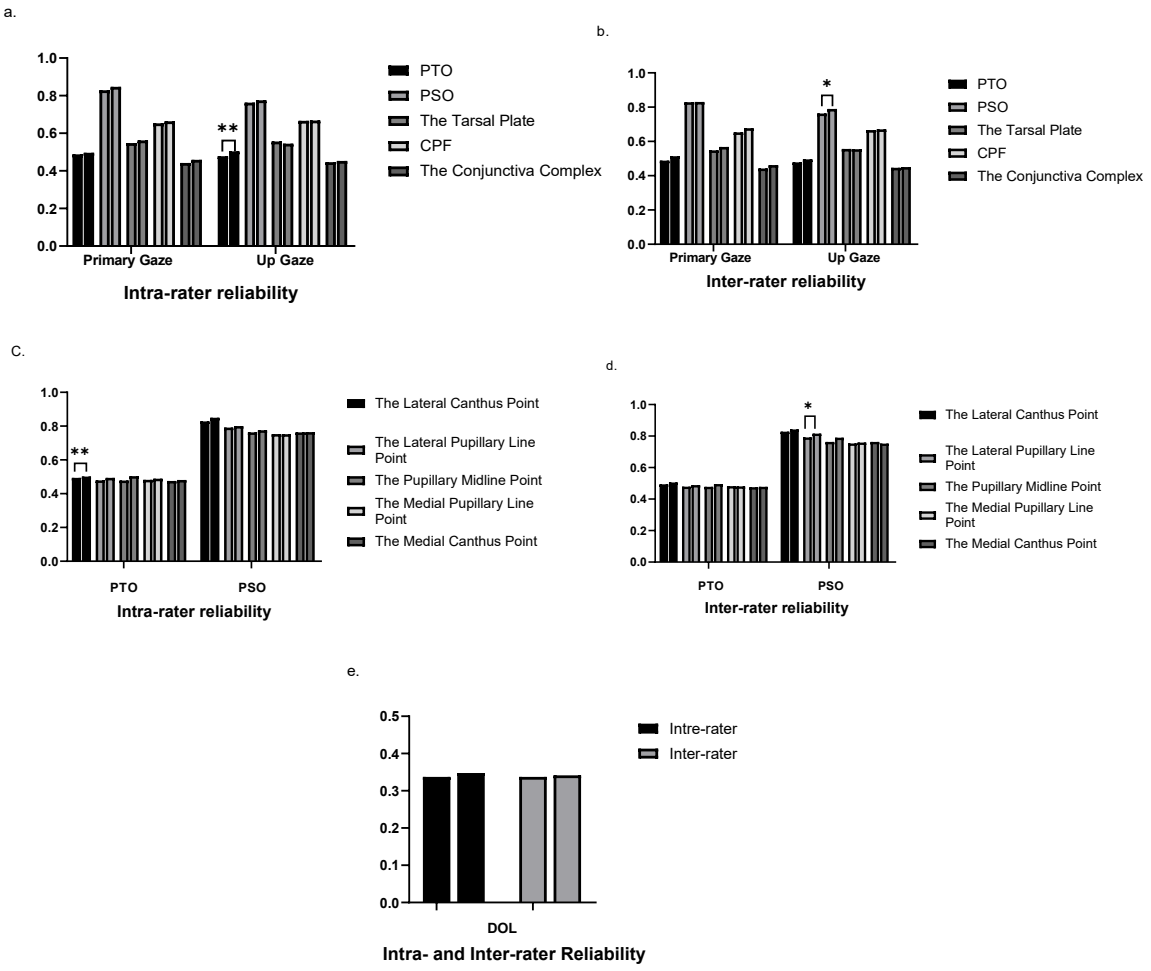

(**Figure 6 a.** The paired t-test for intra-rater at different gaze positions. **b.** The paired t-test for inter-rater at different gaze positions. **c.** The paired t-test for intra-rater at different measurement positions. **d.** The paired t-test for inter-rater at different measurement positions. **e.** The paired t-test for inter-and intra- rater for the thickness of the depressor orbicularis lateralis.) (**p<0.01, *p<0.05)

Therefore, the results of the ICC values and paired t-test indicate that the measurement of the various structures of the lower eyelid by UBM in this study is reliable.

3.2. General Information

In this study, we recruited a total of 42 volunteers (20 males and 22 females) and captured 84 lower eyelid periorbital ultrasound images for further analysis. The age of the volunteers ranged from 18 to 87 years (40.3 ±19.9 years). All results showed no statistically significant differences between the right and left eyes (p>0.05). **Table 2** shows the thickness of each structure of the lower eyelid in different gaze positions.

Table 2. Measurements of Normal Lower Eyelid Structures with Ultrasound Biomicroscope

	PTO	PSO	The Tarsal Plate	CPF	The Conjunctiva Complex
Upgaze Position (mm)	0.50±0.21	0.76±0.19	0.44±0.14	0.55±0.16	0.68±0.18
Primary Position (mm)	0.50±0.18	0.83±0.20	0.45±0.18	0.55±0.15	0.68±0.17
p	0.918	**0.004****	0.525	0.835	0.948

(**Abbreviation: PTO:** pre-tarsal orbicularis. **PSO:** pre-septal orbicularis. **CPF:** the capsulopalpebral fascia.) ** p<0.01

Simultaneously, the height and weight data of all volunteers were analyzed, and the mean BMI measured by all volunteers was 24.16 ± 4.29(range 18-30.7), with no statistical difference compared with the lower eyelid measurement parameters (p>0.05).

Further observation of the ultrasound images, based on the acquired ultrasound real-time images, we observed that the lower eyelid skin and dermis appear as echo-dense linear structures. The lower orbicularis oculi muscle features a long strip-like, hyperechoic structure. The POL, also a part of this muscle, has a similar structure. Based on the anatomical structure, it can be divided into the pre-tarsal orbicularis (PTO) located anteriorly and the pre-septal orbicularis (PSO) located posteriorly. Based on the ultrasound image, it can be observed that

the area of echoes in the PSO is larger than that in the PTO. The tarsal plate and the capsulopalpebral fascia (CPF) appear as a hypoechoic area beneath the orbicularis muscle. The lower eyelid retractor and conjunctival parts are not easily discernible on 50 MHz high-frequency images and can be seen as a complex of the hyperechoic area. (**Figure 7**)

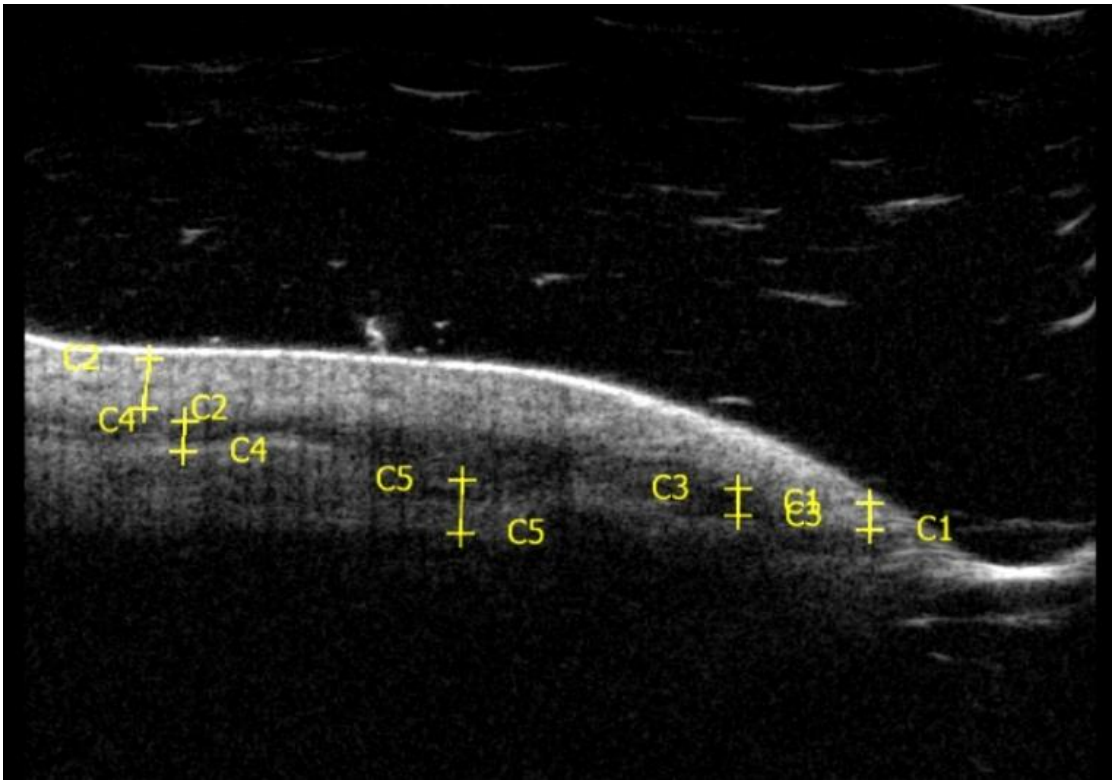

(**Figure 7. C1:** The pre-tarsal orbicularis (PTO). **C2:** The pre-septal orbicularis (PSO). **C3:** The tarsal plate. **C4:** The capsulopalpebral fascia (CPF). **C5**: The conjunctiva complex.)

3.3. Age-related Analysis

Though analyzing the correlation between age and various structure thicknesses of the lower eyelid, it can be found that from the pupillary midline to the medial canthus, the PSO's thickness has a significantly positive correlation with age (p<0.05), that is, the PSO's thickness from the inner side of the lower eyelid (near the nasal side) increases with age. While the thickness of the tarsal plate and CPF also have positive correlations with age (p<0.05).

Similarly, the DOL's thickness, located on the lateral of the orbicularis oculi muscle, also has a positive correlation with age (p<0.05).

In order to derive aging trends by quantifying specific aging-related facial phenotypes in 3D image data,[55] the measured data were further divided into two groups by age (≤30 years old and>30 years old). **Table 3** shows the thickness of PTO and PSO at different measurement points of the lower eyelid and the difference between the two age groups. The PSO thickness was thicker on the lateral side than on the medial side of the eyelid (p<0.01).

Table 3. The Thickness of PTO and PSO at Different Measurement Points of the Lower Eyelid and the Difference between the Two Age Groups.

	PTO					***p***	**PSO**					***p***
	The lateral canthus point	The lateral pupillary line point	The pupillary midline point	The medial pupillary line point	The medial canthus point		The lateral canthus point	The lateral pupillary line point	The pupillary midline point	The medial pupillary line point	The medial canthus point	
Young (≤30 years old) (mm)	0.50±0.14	0.49±0.13	0.47±0.11	0.46±0.13	0.45±0.11	0.089	0.84±0.22	0.79±0.21	0.74±0.18	0.73±0.17	0.70±0.16	**0.000***
Older (＞30 years old) (mm)	0.53±0.20	0.51±0.20	0.54±0.30	0.49±0.18	0.51±0.18	0.445	0.85±0.22	0.85±0.20	0.79±0.19	0.78±0.20	0.82±0.20	0.250
p	0.899	0.552	0.850	0.771	0.337		0.714	0.197	0.220	0.294	**0.02***	

(**Abbreviation: PTO:** pre-tarsal orbicularis. **PSO:** pre-septal orbicularis. **CPF:** the capsulopalpebral fascia.) ** $p<0.01$ * $p<0.05$

3.4. Gaze Position-related Analysis

The thickness of the PSO profile decreased by 7.69% when the eyeball moved from its primary gaze position to an up-gaze position ($p<0.01$). Moreover, the thickness of the eyelid structures did not change significantly in women compared to men when it came to changing the gaze position ($p>0.05$). In dynamic movement, it can be observed that when the gaze position changes from the primary position to the up-gaze position, the hyperechoic area of the orbicularis muscle becomes flat and elongated. In contrast, the rest of the lower eyelid structure does not visually change significantly in the ultrasound image.

For age variation in change of the gaze position, amongst the thickness differences caused by vertical eyeball movement, the conjunctiva complex's thickness and the PSO's thickness in relation to age were negatively correlated ($p<0.01$), and the tarsal plate thickness difference was positively correlated with age ($p<0.01$) (**Figure 8**).

a.

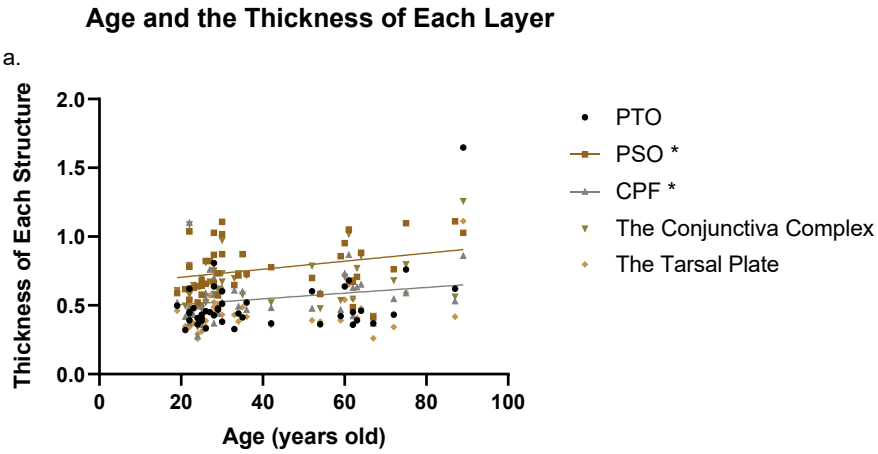
Age and the Thickness of Each Layer
Thickness of Each Structure
2.0
1.5
1.0
0.5
0.0
0
20
40
60
80
100
Age (years old)
PTO
PSO *
CPF *
The Conjunctiva Complex
The Tarsal Plate

b.

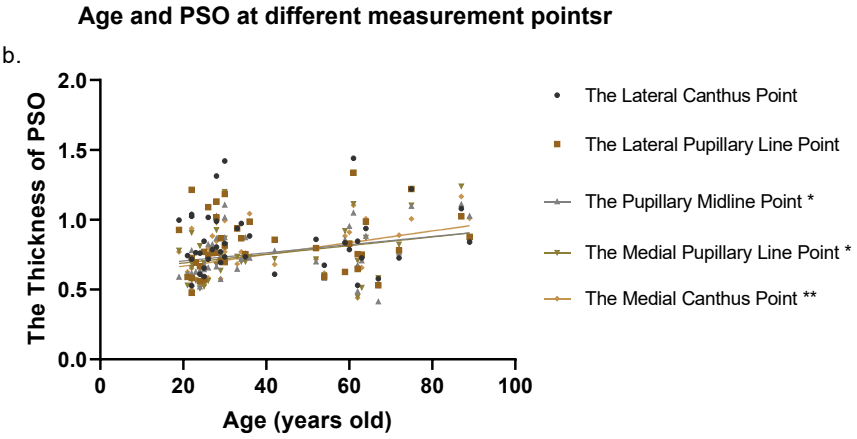
Age and PSO at different measurement pointsr
The Thickness of PSO
2.0
1.5
1.0
0.5
0.0
0
20
40
60
80
100
Age (years old)
The Lateral Canthus Point
The Lateral Pupillary Line Point
The Pupillary Midline Point *
The Medial Pupillary Line Point *
The Medial Canthus Point **

c.

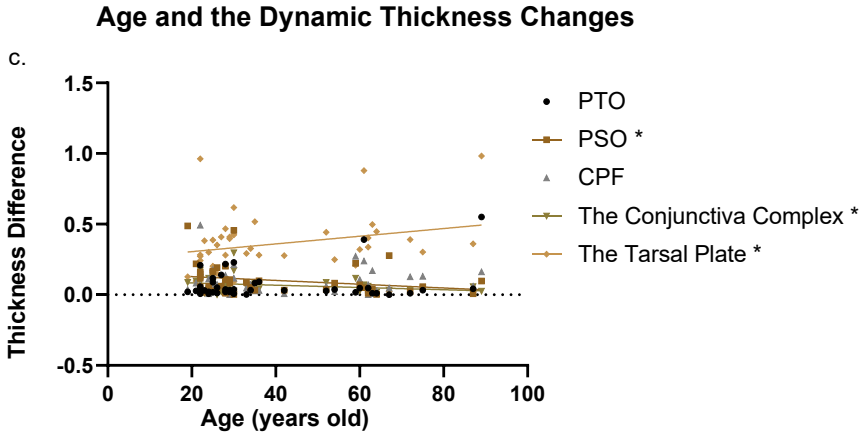
Age and the Dynamic Thickness Changes
Thickness Difference
1.5
1.0
0.5
0.0
-0.5
0
20
40
60
80
100
Age (years old)
PTO
PSO *
CPF
The Conjunctiva Complex *
The Tarsal Plate *

d.


Age and the Thickness of DOL
Thickness of DOL
0.8
0.6
0.4
0.2
0.0
0
20
40
60
80
100
Age (years old)
DOL *

(**Figure 8. a.** The Spearman Correlation Coefficient between the thickness of each layer structure and age (PSO: $r = 0.3660$, $p = 0.0171$. CPF: $r = 0.3743$, $p = 0.0146$). **b.** The Spearman Correlation Coefficient between the PSO's thickness and age (The pupillary midline point: $r = 0.33743$, $p = 0.0146$. The medial pupillary line point: $r = 0.3308$, $p = 0.0324$. The medial canthus line point: $r = 0.4794$, $p = 0.0013$). **c.** The Spearman Correlation Coefficient between the thickness difference and age (PSO: $r = -0.3478$, $p = 0.0240$. The conjunctiva complex: $r = -0.3586$, $p = 0.0197$. The tarsal plate: $r = 0.3255$, $p = 0.0354$). **d.** The Spearman Correlation Coefficient between the thickness of the depressor orbicularis lateralis and age ($r = 0.250$, $p = 0.022$).) ** $p<0.01$ * $p<0.05$

Furthermore, this correlation of PSO and conjunctival complex thickness differences with age was more significant in males ($p<0.01$, $p<0.05$, respectively). For the changes of different gaze directions, in the group of under 30 years old individuals, it can be observed that, when the gaze direction changes from the upper to the primary position, the thickness of PSO changes significantly ($p<0.01$). The statistical results of this study did not indicate a significant difference among the groups of individuals over the age of 30 ($p>0.05$). (**Table 3**)

Table 3. The Thickness of PTO and PSO at Different Measurement Points of the Lower Eyelid and the Difference between the Two Age Groups.

	PTO					***p***	**PSO**					***p***
	The lateral canthus point	The lateral pupillary line point	The pupillary midline point	The medial pupillary line point	The medial canthus point		The lateral canthus point	The lateral pupillary line point	The pupillary midline point	The medial pupillary line point	The medial canthus point	
Young (≤30	0.504±0.14	0.49±0.13	0.47±0.11	0.46±0.13	0.45±0.11	0.0	0.84±0.22	0.79±0.21	0.74±0.18	0.73±0.17	0.70±0.16	0.000**

years old) (mm)						8 9					
Older (>30 years old) (mm)	0.53 ±0.2 0	0.5 1±0 .20	0.5 4±0 .30	0.4 9±0 .18	0.5 1±0 .18	0. 4 4 5	0.85 ±0.2 2	0.85 ±0.2 0	0.79 ±0.1 9	0.78 ±0.2 0	0.82 ±0.2 0	0.2 50
p	0.89 9	0.5 52	0.8 50	0.7 71	0.3 37		0.71 4	0.19 7	0.22 0	0.29 4	0.02 *	

(**Abbreviation: PTO:** pre-tarsal orbicularis. **PSO:** pre-septal orbicularis. **CPF:** the capsulopalpebral fascia.) ** $p<0.01$ * $p<0.05$

4. DISCUSSION

This study demonstrates the feasibility of using UBM to visualize lower eyelid movement. In our study, we determined the changes in the thickness of the lower eyelids' layers during different gaze positions and in different measurement points using UBM. We observed with UBM that when the gaze position changes from the primary position to the up-gaze position, the trajectory of lower eyelid motion under ultrasound usually begins with a subtle elevation of the lower eyelid margin, accompanied by a gradual upward shift of the tarsal plate and associated structures. As vision moves further upward, the lower eyelid moves along a curved trajectory, maintaining a close fit with the eye while maintaining its dynamic range of motion. The results showed that the thickness of PSO decreased significantly from 0.83 ± 0.19 mm to 0.76 ± 0.18 mm when the primary gaze position was shifted to an up-gaze stance (p<0.01). Also, our measured values defined a basic trend in the distribution of the lower eyelid orbicularis muscle, with overall thickness thinning from the lateral to the medial canthus. While the thicknesses of the PTO were 0.51 ± 0.17 mm, 0.48 ± 0.16 mm, 0.50 ± 0.22 mm, 0.48 ± 0.15 mm, and 0.48 ± 0.15 mm, respectively, from the lateral to the medial side; similarly, for the PSO, the thicknesses were 0.85 ± 0.22 mm, 0.82 ± 0.21 mm, 0.76 ± 0.19 mm, 0.75 ± 0.19 mm, and 0.75 ± 0.19 mm. Therefore, it can be seen, that the thicknesses of the lateral PTO, as well as PSO, are thicker than the medial ones (p<0.05, p<0.01, respectively).

4.1. Changes in Gaze Position

The zygomatic and temporal branches of the facial nerve dominate the orbicularis oculi muscle of the lower eyelid, and the interaction between the two branches is mainly responsible for the spontaneous blinking, position of the eyelid, and tension.[56,57] However, the structural changes of the lower eyelid caused by the vertical movement of the eyeball have rarely been reported before. Mohammad et al. [58] tried to use 15MHz ultrasound to analyse the structural changes of the lower eyelid during the vertical movement of the eyeball, mainly observing the changes of the fat pads of the lower eyelid. For our study, we used 50 Hz visual ultrasound to observe more subtle and clear changes in the vertical motion of the layers of the lower eyelid

near the eyelid margin. We found that, when changing from the up-gaze position to the primary position, the mean thickness of the PTO changed from 0.50±0.21 mm to 0.50±0.18 mm, the mean thickness of the PSO increased from 0.76±0.19 mm to 0.83±0.20 mm, and the mean thickness of the tarsal plate increased from 0.44±0.14 mm to 0.45±0.18 mm, the mean thickness of CPF changed from 0.55±0.16 mm to 0.55±0.15 mm, and the mean thickness of the conjunctiva complex changed from 0.68±0.18 mm to 0.68±0.17 mm. It can be observed that the thickness of the PSO changes significantly as the gaze position changes. There are three parts to the orbicularis oculi muscle: the pretarsal portion, which is located in front of the tarsal plates; the pre-septal portion, which is located above the orbital septum; and the orbital portion, which extends eyebrow superiorly and the cheek inferiorly.[59] When the vertical eyeball movements, the different gaze positions also cause changes in the appearance of the lower eyelid, which in turn causes morphological changes in the orbicularis oculi muscle due to changes, thus also suggesting that the appearance of the lower eyelid is strongly correlated with variations in the thickness of the orbicularis oculi muscle.[60] In the relaxed state, the orbicularis oculi is flattened and thinned since the attached portion does not pull on the wing muscles. When squinting, the lower eyelid orbicularis muscle contracts, shortening the vertical width and increasing the thickness. Additionally, we found that this change in the thickness of PSO also changed significantly in the up-gaze and primary position, where the lid fissure became larger and the lower orbicularis muscle relaxed and thinned in upward gaze. In contrast, in the shift from up-gaze to the primary position, the lid fissure became smaller and the muscle contracted and as a result thickened.

4.2. Changes in Age

4.2.1. Age Correlations in Dynamic Changes in Eyelid Structure.

This change in the thickness of the lower eyelid structures due to gaze position is also reflected in age. With age, vertical eyelid movement decreases, which is closely related to the aggravation of eyelid looseness in elderly patients. [61] Our study showed that the lower eyelid structures also respond to eyeball movements accordingly and alter their structures as the

gaze position changes. Interestingly, the effect of vertical eyeball movements on the lower eyelid's thickness is more apparent in young individuals. Also, we observed that the magnitude of changes in PSO and conjunctival thickness were negatively correlated with age amongst the changes in the thickness of various structures when the gaze direction was changed. Then, significant dynamic changes in the lower eyelid are more likely to be observed in young people, and whether this is an age-related change in the elasticity and vitality of muscle and fascial tissue is worth exploring further. During the vertical eyeball saccades procedure, it is believed that the forces transferred to the lower eyelids are carried out through the lower retractor. They have two layers: the capsulolabial fascia and the inferior tarsal muscle.[62] In this up-and-down movement, we found that the PSO and conjunctiva activity changes decreased with age, and conversely, the lower tarsal range of motion increased. Changes in muscle fibers due to aging can reduce muscle tone in facial muscles. However, the increase in connective tissue and the accumulation of fat cells can increase muscle stiffness. [63] Then, this age-related variation, such as muscle fibrosis and increased stiffness, can also affect the orbicularis oculi muscle's contraction force and activity, leading to a decrease in its range of motion. Aging will also lead to conjunctival relaxation and reduced elasticity, thus further reducing the range of its thickness variation. [64] The tarsal plate has a strong tendency to atrophy or shrink with age as observed in previous studies, while aging also exacerbates its structural instability.[65,66] And we speculate that the instability of such a structure causes its thickness to increase in dynamics. Therefore, in the treatment of degenerative entropion, the use of autologous cartilage is more recommended as a "reliable means to restore structural stability".

4.2.2. Age Dependence of Eyelid Structural Thickness

Clinical under-eye bags are defined as bloated and sagging lower eyelid skin that is bilaterally symmetrical and affects the overall aesthetic appearance of the facial features. Patients in the plastic surgery clinic are predominantly middle-aged and older adults over 40 years old, and middle-aged and older patients usually have significant orbicularis oculi muscle laxity. One of the most common morphological changes associated with older facial features is the marked protrusion of the lower eyelid. Few histopathological studies have explored age-

related morphological changes in the orbicularis oculi muscle. Previous studies conducted by MRI imaging analysis revealed that the orbicularis oculi muscle's T1 and T2 imaging increased as people got older, particularly in male subjects. This finding supports the idea that aging can lead to muscle hypertrophy.[67,68] In our study, it was also significant that the thickness of the PSO and CPF increased with age (PSO: r = 0.366, p = 0.017. CPF: r = 0.374, p = 0.015, respectively). This region is representative of the thickness of the inferior orbicularis oculi muscle and the capsulolabial fascia, and hypertrophy and laxity in this region is a major contribution to the formation of "bags" under the eyes. [41,69] Therefore, accurate measurement through this area is helpful for tracking observation in age-related lower eyelid aging, and can be further tried in the treatment and follow-up of lower eyelid rejuvenation surgery.

In our study, we tried to use a 50MHz ultrasonic probe to explore the thickness of DOL and analyse its relationship with age for the first time. For the thickness of DOL measurements, we got that the mean thickness for people aged 30 and under is 0.33±0.08mm, while the mean thickness for people over 30 years old is 0.36±0.10mm. Meanwhile, the thickness of DOL increases with age (p=0.022, r=0.250). According to previous reports, brow ptosis is an aging process in which multiple anatomical structures change under the influence of multiple factors[12,13]. The ptosis of the lateral eyebrows often occurs earlier and to a greater extent than the middle and medial eyebrows. Thus, DOL plays a role in lateral brow ptosis due to aging. When observing the appearance of the human face, we often see the disappearance of the orbital lid grooves in the elderly, and the accumulation of brow bone tissue on the upper eyelid, resulting in swelling of the upper eyelid tissue and ptosis of the outer eyelid. In severe cases,

the appearance of triangular eyes can interfere with facial aesthetics. **(Figure 9)**

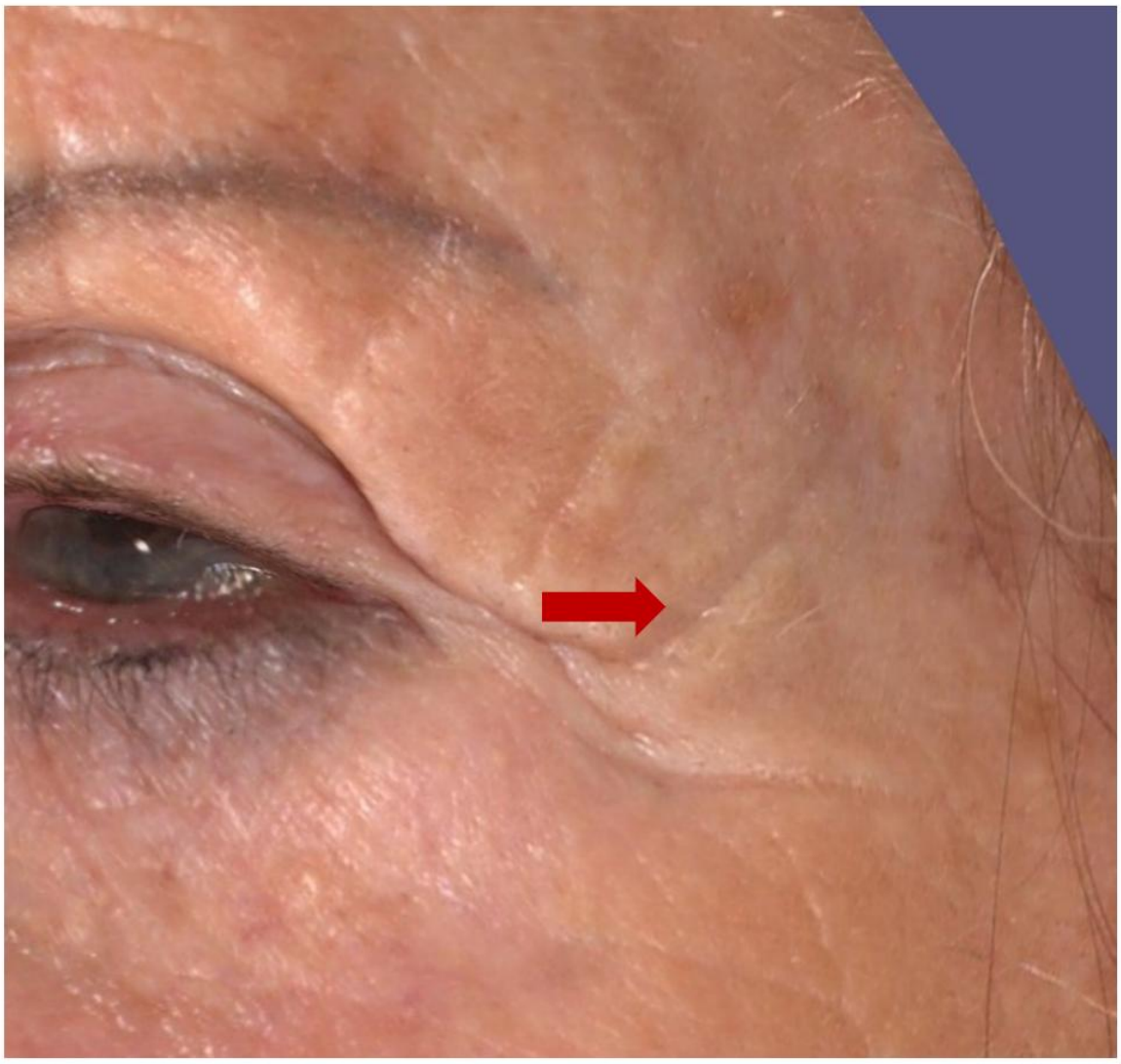

(**Figure 9.** A 75-year-old woman with the depressor orbicularis lateralis (indicated by arrows) and crow′s feet.)

Therefore, we speculate that the thickening of muscles caused by aging may cause changes in appearance. That is, muscle contraction can produce crow's feet radially distributed on the skin outside the orbit. The more hypertrophic and active the muscles are, the more obvious the crow's feet will be [70,71].

4.2.3. Trends in Structural Changes of the Lower Eyelid

We observed the distribution of the thickness of each structure of the lower eyelid through the five measurement points of the lower eyelid. It can be seen that the PSO's thickness shows a gradual thinning trend from the lateral canthus to the medial canthus. Interestingly, we observed a more pronounced increase in the thickness of the PSO at the medial canthus with age, especially in the part of the canthus measured from the mid-pupil line to the medial canthus point. The PSO's thickness at the medial canthus was at 0.70 ± 0.16 mm in individuals below 30 years old and rose to 0.82 ± 0.20 mm in those above 30 years old (p<0.05). The PSO located in the medial canthus is a component of the orbicularis oculi muscle that wraps the lacrimal drainage system, also known as the Horner's muscle.[72] We observed that the thickness of this site increased significantly with age, so we speculated whether the aging of the lacrimal system would also aggravate the muscle hypertrophy and aging of this area.

These structural dynamic changes and thickness distribution variation in relation to age are also reflected in gender. Our study also noted that the dynamic changes exhibited by aging in men more than in women in the lower eyelids' conjunctiva complex and the PSO's active range can be mainly reflected in these structures' dynamic thickness changes (p<0.05, p<0.01, respectively). In contrast, the changes in women are more obvious in the grade of thickness of the tarsal plate (p<0.05). Gherusa H et al.[73] measured the laxity of lower eyelid using a distraction test and found that lower eyelid ectropion, caused by increased horizontal laxity and decreased orbicularis oculi muscle tone, was more pronounced in males. In addition, previous anatomy found that the tarsal plate of males was statistically significantly larger than that of females at the same age.[74] Whether a larger volume can result in a more "stable" structure, thereby limiting the dynamic range of the tarsal plate, we look forward to further exploration. Simultaneously, the age-related changes of PSO thickness distribution can be more reflected in women. We found that the PSO thickness at the medial canthus of female volunteers increased more significantly with age (p<0.05). And as we mentioned in the previous article, whether the age-related thickness change of this part called Horner's muscle

is affected by sex hormones during its aging process while hypertrophy and thickening with age, making it more pronounced in women.

4.3. Reliability and Accuracy of UBM in Eyelid Measurements

As a revolutionary new ultrasound instrument for measuring and observing the structure of the lower eyelid, UBM's reliability in exploring these structures is the basis for all subsequent research. In previous explorations, UBM has been tried and used to measure the structure of a small number of lower eyelid parts. Vasanthapuram et al. [52] used Bland–Altman analysis to analyse the reliability of UBM application when using UBM to measure the lower eyelid. In this study, we utilized the ICC correlation to analyze and determine the reliability of lower eyelid UBM measurements at different measurement points and different gaze positions. We found that the measurement of the primary gaze position of the CPF thickness is slightly less reliable in intra- and inter-reliability than in other structures, which may be related to the blurred boundary of the ultrasound echo of the CPF, resulting in a large error. The remaining reliability reached an excellent agreement, proving the reliability of UBM in the measurement of dynamic changes of the lower eyelid. Simultaneously, we performed a re-evaluation of the lower eyelid UBM results with a paired t-test. We found less agreement between PTO and PSO thickness measurements when gazing upward. The measurements there were in agreement with the primary gaze position. We hypothesized that capturing clear ultrasound images during the up-gaze position is more difficult than during primary gaze due to the need to ask the volunteer to fixate on a gaze point above the head for gazing, which can be challenging for image acquisition. Therefore, we suggest that a more evident gaze point can be assigned to assist the patient in maintaining ocular position, and simultaneously taking multiple, repeated measurements can minimize this discrepancy.

4.4. Limitations

This study acknowledges several noteworthy limitations that warrant consideration. Primarily, the utilization of ultrasonic biomicroscopy (UBM) for measurement relies on the thickness of the lower eyelid, a parameter subjected to inherent variability. While ICC analysis

and paired t-test were employed to assess reliability, the scarcity of imaging data pertaining specifically to the lower eyelid poses a challenge. Integration with comprehensive anatomical research could enhance the precision and validity of our findings. Additionally, the scope of our investigation was constrained by the examination of a relatively small cohort of volunteers, which may restrict the generalizability of the results. Notably, the composition of the participant pool predominantly comprised individuals of Caucasian descent, thus limiting the extent to which our conclusions can be extrapolated across diverse ethnic populations. Addressing these limitations through expanded sample sizes and broader demographic representation would undoubtedly fortify the robustness and applicability of future studies in this domain.

5. CONCLUSIONS

In this study, we took advantage of the noninvasive, convenient features of UBM to visually characterize the echogenicity and thickness of normal lower eyelid structures. Our measurements of the lower eyelid by UBM revealed that the various structures of the lower eyelid are correlated with age and the direction of eyeball movement to varying degrees. Therefore, UBM is a reliable, efficient, and time-saving alternative method for imaging the structures of the lower eyelid, which can be used to study anatomical differences between different races and individuals, dynamically and locally display eyelid structures, and has potential uses, and in disease and preoperative evaluation of lower eyelid structures.

6. REFERENCES

1. American Academy of Ophthalmology. https://anatomy.co.uk/eyelid/.
2. Kakizaki H, Malhotra R, Madge SN, Selva D. Lower Eyelid Anatomy: An Update. 2009; **63**(3): 344-51.
3. Roh MR, Chung KY. Infraorbital dark circles: definition, causes, and treatment options. Dermatologic surgery : official publication for American Society for Dermatologic Surgery [et al] 2009; **35**(8): 1163-71.
4. Holly FJ. Tear film physiology. American journal of optometry and physiological optics 1980; **57**(4): 252-7.
5. Evinger C, Shaw M, Peck C, Manning K, Baker RJJon. Blinking and associated eye movements in humans, guinea pigs, and rabbits. 1984; **52**(2): 323-39.
6. Becker W, Fuchs AFJJon. Lid-eye coordination during vertical gaze changes in man and monkey. 1988; **60**(4): 1227-52.
7. Cochran ML LM, Czyz CN. Anatomy, Head and Neck: Eyelid. 2023 Aug 14 https://www.ncbi.nlm.nih.gov/books/NBK482304/2024).
8. Choi Y, Kang HG, Nam YS, Kang JG, Kim IB. Facial Nerve Supply to the Orbicularis Oculi around the Lower Eyelid: Anatomy and Its Clinical Implications. Plastic and reconstructive surgery 2017; **140**(2): 261-71.
9. Evan H. Black FAN, Christopher J. Calvano, Geoffrey J. Gladstone, Mark R. Levine. Smith and Nesi's Ophthalmic Plastic and Reconstructive Surgery. 3rd edition ed; 2012.
10. Malena M. Amato BMJWS. Duane's Ophthalmology 2006. http://www.oculist.net/downaton502/prof/ebook/duanes/pages/v5/v5c072.htmlChapter 72).
11. Tong J, Lopez MJ, Patel BC. Anatomy, Head and Neck: Eye Orbicularis Oculi Muscle. StatPearls. Treasure Island (FL) ineligible companies. Disclosure: Michael Lopez declares no relevant financial relationships with ineligible companies. Disclosure: Bhupendra Patel declares no relevant financial relationships with ineligible companies.: StatPearls Publishing
Copyright © 2024, StatPearls Publishing LLC.; 2024.
12. Lemke BN, Stasior OG. The anatomy of eyebrow ptosis. Archives of ophthalmology (Chicago, Ill : 1960) 1982; **100**(6): 981-6.
13. Tamatsu Y, Tsukahara K, Shimada K. Findings of unique small muscle fibers at the superficial portion of the orbicularis oculi in the lateral canthal region of Japanese adult cadavers. Clinical anatomy (New York, NY) 2010; **23**(6): 637-41.
14. Hwang K. Surgical anatomy of the lower eyelid relating to lower blepharoplasty. Anatomy & cell biology 2010; **43**(1): 15-24.
15. Anastassov GE, St Hilaire H. Periorbital and midfacial rejuvenation via blepharoplasty and sub-periosteal midface rhytidectomy. International journal of oral and maxillofacial surgery 2006; **35**(4): 301-11.
16. Bron AJ, Benjamin L, Snibson GR. Meibomian gland disease. Classification and grading of lid changes. Eye (London, England) 1991; **5 (Pt 4)**: 395-411.
17. Aumond S, Bitton E. The eyelash follicle features and anomalies: A review. Journal of optometry 2018; **11**(4): 211-22.
18. Honavar SG, Manjandavida FP. Recent Advances in Ophthalmic Plastic Surgery: Part 1-Eyelid. Asia-Pacific journal of ophthalmology (Philadelphia, Pa) 2013; **2**(5): 328-40.
19. Mukarram M, Khachemoune A. Upper and Lower Eyelid Malignancies: Differences in Clinical Presentation, Metastasis, and Treatment. Archives of dermatological research 2024; **316**(7): 429.
20. Bedrossian EJDsfoco, ocular anatomy, embryology, teratology. Embryology and anatomy of the eyelid. 2004; **1**: 1-24.
21. Huang LC, Jean D, Proske RJ, McDermott AM. Innate Immunity at the Ocular Surface: Spectrum of Antimicrobial Peptide Expression. Investigative Ophthalmology & Visual Science 2005; **46**(13): 883-.

22. Shumway CL, Motlagh M, Wade M. Anatomy, Head and Neck, Eye Conjunctiva. StatPearls. Treasure Island (FL) ineligible companies. Disclosure: Mahsaw Motlagh declares no relevant financial relationships with ineligible companies. Disclosure: Matthew Wade declares no relevant financial relationships with ineligible companies.: StatPearls Publishing
Copyright © 2024, StatPearls Publishing LLC.; 2024.
23. Steuhl KP. Ultrastructure of the conjunctival epithelium. Developments in ophthalmology 1989; **19**: 1-104.
24. Ting M, Ezra DG. Unravelling the Complex Anatomy of the Tear Trough and Lower Eyelid Folds: A Review of Cadaveric Studies in the Literature. The Journal of craniofacial surgery 2022; **33**(8): 2670-6.
25. Kakizaki H, Chan W, Madge SN, Malhotra R, Selva D. Lower eyelid retractors in Caucasians. Ophthalmology 2009; **116**(7): 1402-4.
26. Slaoui M, Bauchet A-L, Fiette L. Tissue Sampling and Processing for Histopathology Evaluation. 2017: 101-14.
27. Carter SR, Seiff SR, Grant PE, Vigneron DB. The Asian lower eyelid: a comparative anatomic study using high-resolution magnetic resonance imaging. Ophthalmic plastic and reconstructive surgery 1998; **14**(4): 227-34.
28. Osaki T, Murakami H, Tamura R, Nomura T, Hashikawa K, Terashi H. Analysis of Orbital Morphology and its Relationship With Eyelid Morphology. The Journal of craniofacial surgery 2020; **31**(7): 1875-8.
29. Damasceno RW, Avgitidou G, Belfort R, Jr., Dantas PE, Holbach LM, Heindl LM. Eyelid aging: pathophysiology and clinical management. Arquivos brasileiros de oftalmologia 2015; **78**(5): 328-31.
30. R. Eyelid aging: pathophysiology and clinical management. 2015; **78**(2015).
31. Guinot C, Malvy DJ, Ambroisine L, et al. Relative contribution of intrinsic vs extrinsic factors to skin aging as determined by a validated skin age score. Archives of dermatology 2002; **138**(11): 1454-60.
32. Nagi KS, Carlson JA, Wladis EJ. Histologic assessment of dermatochalasis: elastolysis and lymphostasis are fundamental and interrelated findings. Ophthalmology 2011; **118**(6): 1205-10.
33. Montes GS. Structural biology of the fibres of the collagenous and elastic systems. Cell biology international 1996; **20**(1): 15-27.
34. Kielty CM, Sherratt MJ, Shuttleworth CA. Elastic fibres. Journal of cell science 2002; **115**(Pt 14): 2817-28.
35. Kahn DM, Shaw RB. Overview of current thoughts on facial volume and aging. Facial Plast Surg 2010; **26**(5): 350-5.
36. Yapa S, Raghavan U. Lower Eyelid Transcutaneous Blepharoplasty, Minimizing Complications and Correction of Lower Eyelid Malposition. Facial Plast Surg 2023; **39**(1): 8-19.
37. Buchanan DR, Wulc AE. Contemporary thoughts on lower eyelid/midface aging. Clinics in plastic surgery 2015; **42**(1): 1-15.
38. Cho C, Cho E, Kim N, et al. Age-related biophysical changes of the epidermal and dermal skin in Korean women. Skin research and technology : official journal of International Society for Bioengineering and the Skin (ISBS) [and] International Society for Digital Imaging of Skin (ISDIS) [and] International Society for Skin Imaging (ISSI) 2019; **25**(4): 504-11.
39. Farage M, Miller K, Maibach H. Textbook of Aging Skin; 2010.
40. Holds JB. Lower eyelid blepharoplasty: a procedure in evolution. Missouri medicine 2010; **107**(6): 391-5.
41. Goldberg RA, McCann JD, Fiaschetti D, Ben Simon GJ. What causes eyelid bags? Analysis of 114 consecutive patients. Plastic and reconstructive surgery 2005; **115**(5): 1395-402; discussion 403-4.
42. Pavlin CJ, Sherar MD, Foster FS. Subsurface ultrasound microscopic imaging of the intact eye. Ophthalmology 1990; **97**(2): 244-50.

43. Kooner KS, Zimmerman TJ. Pearls in glaucoma management. Annals of ophthalmology 1984; **16**(6): 507, 9.
44. He M, Wang D, Jiang Y. Overview of Ultrasound Biomicroscopy. Journal of current glaucoma practice 2012; **6**(1): 25-53.
45. Berens C, Breakey AS, Carter GZ. A pocket flashlight with interchangeable tips designed especially for eye examinations. American journal of ophthalmology 1956; **42**(3): 488-9.
46. Baum G, Greenwood I. The application of ultrasonic locating techniques to ophthalmology. II. Ultrasonic slit lamp in the ultrasonic visualization of soft tissues. AMA archives of ophthalmology 1958; **60**(2): 263-79.
47. Silverman RH. High-resolution ultrasound imaging of the eye - a review. Clinical & experimental ophthalmology 2009; **37**(1): 54-67.
48. Mansoori T. Qualitative ultrasound biomicroscopy of the normal anterior segment. Indian journal of ophthalmology 2023; **71**(5): 2323.
49. Pavlin CJ, Harasiewicz K, Foster FS. Ultrasound biomicroscopy of anterior segment structures in normal and glaucomatous eyes. American journal of ophthalmology 1992; **113**(4): 381-9.
50. Pavlin CJ, Foster FS. Ultrasound biomicroscopy in glaucoma. Acta ophthalmologica Supplement 1992; (204): 7-9.
51. Vasanthapuram VH, Naik MN. Lower eyelid entropion in thyroid eye disease. Orbit 2022; **41**(3): 335-40.
52. Vasanthapuram VH, Saha P, Mohamed A, Naik MN. Ultrasound biomicroscopic features of the normal lower eyelid. Orbit 2021; **40**(5): 375-80.
53. Ju X, Kowanz D, Guo Y, et al. Dynamic Measurement and Analysis of Upper Eyelid Changes Using Ultrasound Biomicroscopy. Ultrasound in medicine & biology 2024; **50**(8): 1240-6.
54. Kikkawa DO, Ochabski R, Weinreb RN. Ultrasound biomicroscopy of eyelid lesions. Ophthalmologica Journal international d'ophtalmologie International journal of ophthalmology Zeitschrift fur Augenheilkunde 2003; **217**(1): 20-3.
55. Chen W, Qian W, Wu G, et al. Three-dimensional human facial morphologies as robust aging markers. Cell Research 2015; **25**(5): 574-87.
56. Caminer DM, Newman MI, Boyd JB. Angular nerve: new insights on innervation of the corrugator supercilii and procerus muscles. Journal of plastic, reconstructive & aesthetic surgery : JPRAS 2006; **59**(4): 366-72.
57. Choi Y, Kang HG, Nam YS, Kang J-G, Kim I-B. Facial Nerve Supply to the Orbicularis Oculi around the Lower Eyelid: Anatomy and Its Clinical Implications. 2017; **140**(2): 261-71.
58. Rajabi MT, Papageorgiou K, Chang SH, et al. Ultrasonographic visualization of lower eyelid structures and dynamic motion analysis. International journal of ophthalmology 2013; **6**(5): 592-5.
59. Jafer Chardoub AA, Patel BC. Eyelid Myokymia. StatPearls. Treasure Island (FL): StatPearls Publishing
Copyright © 2023, StatPearls Publishing LLC.; 2023.
60. Cruz AA, Távora DB, Martin LF. Effect of eyelid saccades on the position of lateral canthus in young and older subjects. Orbit 2008; **27**(1): 1-4.
61. Shore JW. Changes in lower eyelid resting position, movement, and tone with age. Am J Ophthalmol 1985; **99**(4): 415-23.
62. Kakizaki H, Zhao J, Nakano T, et al. The lower eyelid retractor consists of definite double layers. Ophthalmology 2006; **113**(12): 2346-50.
63. Ramazanoglu E, Turhan B, Usgu S. Age Related Changes of Superior Orbicularis Oris Muscle in Terms of Tone and Viscoelastic Properties. Journal of Craniofacial Surgery 2022; **33**(1).
64. Marmalidou A, Kheirkhah A, Dana R. Conjunctivochalasis: a systematic review. Surv Ophthalmol 2018; **63**(4): 554-64.

65. Huang TT, Amayo E, Lewis SR. A histological study of the lower tarsus and the significance in the surgical management of a involutional (senile) entropion. Plastic and reconstructive surgery 1981; **67**(5): 585-90.
66. Bashour M, Harvey J. Causes of involutional ectropion and entropion--age-related tarsal changes are the key. Ophthalmic Plast Reconstr Surg 2000; **16**(2): 131-41.
67. Watanabe M, Buch K, Fujita A, Christiansen CL, Jara H, Sakai O. MR relaxometry for the facial ageing assessment: the preliminary study of the age dependency in the MR relaxometry parameters within the facial soft tissue. Dento maxillo facial radiology 2015; **44**(7): 20150047.
68. Lee H, Park M, Lee J, Lee ES, Baek S. Histopathologic findings of the orbicularis oculi in upper eyelid aging: total or minimal excision of orbicularis oculi in upper blepharoplasty. Archives of facial plastic surgery 2012; **14**(4): 253-7.
69. Coban I, Derin O, Sirinturk S, Pinar Y, Govsa F. Anatomical Basis for the Lower Eyelid Rejuvenation. Aesthetic Plast Surg 2023; **47**(3): 1059-66.
70. Fogli A. [Orbicularis oculi muscle and crow's feet. Pathogenesis and surgical approach]. Annales de chirurgie plastique et esthetique 1992; **37**(5): 510-8.
71. Matarasso SL, Matarasso A. Treatment guidelines for botulinum toxin type A for the periocular region and a report on partial upper lip ptosis following injections to the lateral canthal rhytids. Plastic and reconstructive surgery 2001; **108**(1): 208-14; discussion 15-7.
72. Ali MJ, Paulsen F. Horner's Muscle or Horner-Duverney's Muscle. Ophthalmic Plast Reconstr Surg 2020; **36**(2): 208.
73. Milbratz-Moré GH, Pauli MP, Lohn CLB, Pereira FJ, Grumann AJ. Lower Eyelid Distraction Test: New Insights on the Reference Value. Ophthalmic Plast Reconstr Surg 2019; **35**(6): 574-7.
74. Farkas LG. Anthropometry of the head and face. 2nd Ed ed. New York: Raven Press; 1994.

7. APPENDIX

7.1. List of Figures

7.2. List of Tables

8. PUBLICATIONS

1. **Ju X**, Gaca P, Fan W, Rokohl AC, Guo Y, Wawer Matos PA, Emmert S, Kakkassery V, Heindl LM. Therapy Failure and Resistance Mechanism in Eyelid and Ocular Surface Tumors. Neurosignals. 2022 Aug 25;30(S1):21-38. doi: 10.33594/000000560. PMID: 36005157.

2. **Ju X**, Rokohl AC, Fan W, Ukehajdaraj N, Wawer Matos PA, Guo Y, Heindl LM. Changes in Periocular Asymmetry by Age and Gender: A Three-Dimensional Photogrammetry Study in a Caucasian Population. Facial Plast Surg Aesthet Med. 2024 Apr 3. doi: 10.1089/fpsam.2023.0282. Epub ahead of print. PMID: 38569156.

3. **Ju X**, Rokohl AC, Li X, Guo Y, Yao K, Fan W, Heindl LM. A UV-related risk analysis in ophthalmic malignancies: Increased UV exposure may cause ocular malignancies. Adv Ophthalmol Pract Res. 2024 Apr 5;4(2):98-105. doi: 10.1016/j.aopr.2024.04.001. PMID: 38707995; PMCID: PMC11066588.

4. **Ju X**, Kowanz D, Guo Y, Li X, Wawer Matos PA, Fan W, Rokohl AC, Heindl LM. Dynamic Measurement and Analysis of Upper Eyelid Changes Using Ultrasound Biomicroscopy. Ultrasound Med Biol. 2024 May 27: S0301-5629(24)00190-X. doi: 10.1016/j.ultrasmedbio.2024.04.014. Epub ahead of print. PMID: 38806337.

5. **Ju X**, Rokohl AC, Fan W, Simon M, Li X, Hou X, Ukehajdaraj N, Wawer Matos PA, Guo Y, Heindl LM. Periocular Asymmetry Index in Caucasian Populations Using Three-dimensional Photogrammetry Assessment. Aesthetic Plast Surg. 2024 May 28. doi: 10.1007/s00266-024-04125-8. Epub ahead of print. PMID: 38806825.